

## Mathematical Modeling of blood flow in the artery with a reference to rupture behavior of Stenosis

V.K. Katiyar<sup>1</sup>, K.S. Basavarajappa<sup>2</sup>, Ashwini M Rao<sup>3</sup>

1. Department of Mathematics, Indian Institute of Technology, Roorkee
2. Department of Mathematics, Bapuji Institute of Engineering and Technology, Davangere
3. Department of Mathematics, Bapuji Institute of Engineering and Technology, Davangere

### Abstract

*The study concerns the estimation of rupture behavior of mild stenosis with a reference to mathematical modeling. The increase of growth of Stenosis size leading to the rupture (peak) stage which gives the evidence to compare with calcification inside the aortic valve. The opening at this location will be an area as  $5\text{mm} \times 2\text{mm}$  which is predicted slightly higher than the regular diameter of the artery at that location. Fluctuating pressures cause instabilities which in turn the nature of turbulence at the rupture of stenosis can be detected. In the present study the flow under consideration is laminar. The increase in peak systolic blood pressure will be around  $30\text{ mm Hg}$  because of  $\delta > 0.55\text{mm}$  with the corresponding systolic velocity as  $62.3\text{ cm/sec}$  when the growth is at  $\delta < 0$ . The effect of different wave forms, stream functions velocity field, average volume flow rate, pressure gradient and the wall shear stress have been analysed. The velocity gradient at the wall referred to as wall shear rate is larger than the one calculated in the arteries of different diameters. The large shear rate in the distal part of the stenosis causes a great shearing action on the inner surface of the wall. Series solution method is employed in the analysis to quantify the velocity in the axial direction, flow rate and the wall shear stress at the varying location of the stenosis near to rupture stage and compared [2], [3],[5],[6].*

**Key words:** stenosis, calcification, rupture.

### Address for Correspondence:

Dr. K.S.Basavarajappa,  
Professor and Head,  
Department of Mathematics,  
Bapuji Institute of Engineering and Technology, Davangere-04  
Email: ksbraju@hotmail.com

## Introduction

The arterial diseases have major impact on medical diagnosis. The common form of arterial narrowing (Stenosis) is caused by the deposition of fats and fibrous tissues in the arterial wall. Effect of the stenosis decreases the requirement of blood to the regions beyond the narrowing region. Analysis of mild stenosis is being carried out with a view of viscosity variation of blood using mathematical modelling. The hematocrit of RBC changes from (I) 42% to 45% and (II) 34% to 42% as, viscosity varies from 3.0 cp to 3.3 cp, Here the case (I) occurs when there is an increase of wall shear stress in relation to the increase of shear stress at the apex of the branch of the main artery. The radius of mild stenosed artery will be in terms of variation of axial coordinates at the initial position of the growing stenosis and the size by 0.5 mm as another thickness. Mathematical formulation for the mild stenosed artery is considered in terms of varying thickness of the stenosis ( $\delta$ ). This is due to the increase of viscosity sets the increase of arterial blood pressure rate by 5 mm Hg (the initial value). The rupture due to the irregular growth of stenosis is studied when the diameter of the size of the stenosis increases.

Many studies have shown the conclusive remarks both analytically and experimentally. Their remarks indicate the study of physiological flow parameters for the growth of stenosis such as blood velocity, flow rate and pressure drop across the stenosis. But the profiles of velocity and the flow rate, the pressure drop exhibit the blunting effect when the flow is studied for mild stenosis in coronary artery with irregular growth of stenosis.

Back et. al [1] made an experimental study on mild stenosis to estimate the pressure drop in the narrowing region. Liepsch et al., [4] discussed velocity measurements in true-to-scale silicon rubber model of the aortic arch using Laser-Doppler anemometer. Katiyar [6] analyzed the pulsatile flow of blood in an elastic tube with wall deformation. David Steinmen et al. [7] explained the flow patterns at the stenosed carotid bifurcation on effect of concentric versus eccentric stenosis. Basavarajappa et al. [8] studied the experimental and numerical analysis of pulsatile flow in carotid artery bifurcations. J.C. Mishra et. al [9] discussed peristaltic motion of blood in the microcirculatory system. It is revealed that velocity of blood and wall shear stress is appreciably affected due to the non uniform geometry of blood vessels.

With a view of quantitative study of the viscosity variation of blood, mathematical model is proposed to assess the increase of focal point of parabolic flow on the horizontal axis when the axisymmetric flow is under analytical consideration. It is assumed that the mild stenosis could be represented by a smooth mathematical function as the cosine curve which is not the general case. The case of irregular growth of stenosis ( $\delta > 0.55\text{mm}$ ) is considered with the arterial flow increased by 4 mm Hg at an aortic velocity of 100cm/sec. This causes the unsteady nature of flow. The increase of systolic pressure accelerated and ventricular pressure becomes lower than aortic one. At the region with stenosed the velocity may be greatly increased with a corresponding drop in pressure. Further fluctuations in pressure will appear in the diastolic blood pressure. The clinical observation of variation of velocity, flux, pressure fluctuations gives the insight to study the rupture case of aneurysm. An attempt has been made in the present study to quantify theoretically the peak diastolic pressure fluctuations when the peak velocity (up to 200cm/sec) is under consideration. The increase of growth of stenosis size leading to the rupture (peak) stage will give the evidence to compare with calcification inside the aortic valve (the opening at this location will be an area as 5mm  $\times$  2mm which is slightly

higher than the regular diameter of the artery at that location). Fluctuating pressures cause instabilities which in turn the nature of turbulence at the rupture of stenosis can be detected. In the present study the flow under consideration is laminar. The peak systolic blood pressure will be around 30 mm Hg because of  $\delta > 0.55mm$  with the corresponding systolic velocity as 62.3 cm/sec when the growth is at  $\delta < 0.25mm$ . The computations including the effect of different wave forms, stream functions velocity field, average volume flow rate, pressure gradient and the wall shear stress.

### Formulation

Hemodynamic effects referring by a mild stenosis are studied by expressing the radius as cosine curve. It consists of the initial radius, the initial thickness of the stenosed region, the rupture coefficient and axial distances in the flow directions. The flow direction under consideration will be for downstream and upstream of the vessel segment. The blood is considered to be viscous and incompressible.

$$R(z) = R_0 - \frac{m\delta_v}{2} \left[ 1 + \cos\left(\frac{\pi(z - z_i)}{z_0}\right) \right] \quad (1)$$

Where  $R_0$  – initial radius of the stenosed area

$\delta_v$  – thickness of the stenosed region

$z$  – axial distance

$z_0$  – initial axial distance

$z_i$  - axial distance at  $i = 0.2, 0.4, 0.6, 0.8$

The rupture coefficient 'm' has been modeled as

$$m = \frac{1}{4096} \frac{G_0 D^4}{\vartheta^2 \rho} \quad (2)$$

Here  $G_0$  – enhanced diastolic pressure,  $D$  – Diameter,  $\vartheta$  – kinematic viscosity,  $\rho$  – density

The flow is considered to be laminar, steady and isothermal. Navier Stokes equations have been formulated to compute velocity of radial ( $r$ ), amplitude ( $\theta$ ) and axial ( $z$ ) components (for conservation of flow) describe the axisymmetric flow for the case of stenosis are given by

$$r \text{ component: } \rho \left[ \frac{\partial v_r}{\partial t} - \frac{v_\theta^2}{r} \right] = \rho f_r - \frac{\partial p}{\partial r} + \mu \left[ \nabla^2 v_r - \frac{v_r}{r^2} - \frac{2}{r^2} \frac{\partial v_\theta}{\partial \theta} \right] \quad (3)$$

$$\theta \text{ component: } \rho \left[ \frac{\partial v_\theta}{\partial t} + \frac{v_r v_\theta}{r} \right] = \rho f_\theta - \frac{1}{r} \frac{\partial p}{\partial \theta} + \mu \left[ \nabla^2 v_\theta + \frac{2}{r^2} \frac{\partial v_r}{\partial \theta} - \frac{v_\theta}{r^2} \right] \quad (4)$$

$$z \text{ component: } \rho \frac{\partial v_z}{\partial t} = \rho f_z - \frac{\partial p}{\partial z} + \mu \nabla^2 v_z \quad (5)$$

$$\frac{1}{r} \frac{\partial}{\partial r} (r v_r) + \frac{1}{r} \frac{\partial v_\theta}{\partial \theta} + \frac{\partial v_z}{\partial z} = 0 \quad (6)$$

Boundary Conditions for the case of right angle constriction with a reference to rupture case between 50% to 86% are

$$\text{At } r = 0, \frac{\partial v}{\partial r} = 0,$$

$$u = \max \text{ at } r = R = a \quad (7)$$

$$y = 0, u = 0, y = y_0, u = U \quad (8)$$

### No Slip Condition

$$v_r = v_z = 0 \text{ at } r = R(Z) \quad (9)$$



**Normalization**

$$x_i^* = \frac{x_i}{l_0}, v_i^* = \frac{v_i}{u_0}, t^* = \frac{tu_0}{l_0}, \rho^* = \frac{\rho}{\rho_0}, \mu^* = \frac{\mu}{\mu_0}, p^* = \frac{p}{p_0}, \tau^* = \frac{\tau}{\tau_0}, k^* = \frac{k}{k_0},$$

$$c_p^* = \frac{c_p}{c_{p0}}, R^* = \frac{R\rho_0 T_0}{p_0}, \vartheta^* = \frac{\vartheta}{\vartheta_0}, D^* = \frac{LD}{D_0}, f_i^* = \frac{f_i}{f_0} \quad (10)$$

where the quantities with the subscripts "0" are initial reference values associated with the flow.

r component: 
$$\rho \left[ \frac{\partial v_r^*}{\partial t} - \frac{v_\theta^{*2}}{r} \right] = \rho^* f_r^* - \frac{\partial p^*}{\partial r} + \mu^* \left[ \nabla^2 v_r^* - \frac{v_r^*}{r^2} - \frac{2}{r^2} \frac{\partial v_\theta^*}{\partial \theta} \right] \quad (11)$$

θ component: 
$$\rho \left[ \frac{\partial v_\theta^*}{\partial t} + \frac{v_r^* v_\theta^*}{r} \right] = \rho^* f_\theta^* - \frac{1}{r} \frac{\partial p^*}{\partial \theta} + \mu^* \left[ \nabla^2 v_\theta^* + \frac{2}{r^2} \frac{\partial v_r^*}{\partial \theta} - \frac{v_\theta^*}{r^2} \right] \quad (12)$$

z component: 
$$\rho \frac{\partial v_z^*}{\partial t} = \rho^* f_z^* - \frac{\partial p^*}{\partial z} + \mu^* \nabla^2 v_z^* \quad (13)$$

Introducing three perturbations  $m_1, m_2, m_3$  to describe the rupture behavior of the stenosis

$$m_i = \frac{1}{4096} \frac{G_0 D^4}{\vartheta^{*2} \rho^*} \quad (14)$$

**Analysis and Numerical Computation**

The plaque growth is along the artery wall. The wall movement due to increase in the velocity of blood gets perturbed and the boundary conditions applied to equations (3), (4), (5) and (6) give the velocity in radial and axial directions ( $v_r$  and  $v_z$ ) only. The elastic properties along the length of the stenosis as well as in the unobstructed portion are taken for the case of rupture stage such that the minimum diameter ( $\delta = 0.55\text{mm}(71\%)$ ) of stenosis and to the maximum diameter ( $\delta = 0.853\text{mm}(93.14\%)$ ) so that the wave speed rapidly increases before rupture and collapses after rupture. This is because, the stenotic region which undergoes to the highest stress which in turn influences to cause the high occlusion at the upstream of the stenotic region. As a result the larger shear rate effects the fluctuation of the inner surface of the wall of the artery. Consequently the velocity gradient at the wall also refer to as wall shear rate which will be larger than the one calculated in the rest of the vessel.

(transmural pressures  $\frac{\partial p}{\partial r} \approx 0, \frac{\partial p}{\partial \theta} \approx 0$  and  $\frac{\partial p}{\partial z} \approx 0$ )

To solve for  $v_r$  we assume  $\frac{\partial p}{\partial r} = 0$  (the transmural pressure) at the rupture stage of the stenosis. Thus velocity in radial and axial directions are computed as,

$$\frac{\partial^2 v_r}{\partial r^2} + \frac{1}{r} \frac{\partial v_r}{\partial r} - \frac{v_r}{r^2} + \frac{\partial^2 v_r}{\partial z^2} = 0 \quad (15)$$

We obtain in the similar type ( $\frac{\partial p}{\partial \theta} \approx 0$  at the rupture stage) for  $v_\theta$

$$\frac{\partial^2 v_\theta}{\partial r^2} + \frac{1}{r} \frac{\partial v_\theta}{\partial r} + \frac{1}{r^2} \frac{\partial^2 v_\theta}{\partial \theta^2} + \frac{1}{r^2} \frac{\partial^2 v_\theta}{\partial z^2} - \frac{1}{r^2} v_\theta = 0 \quad (16)$$

$$\frac{\partial}{\partial r} \left( r \frac{\partial v_z}{\partial r} \right) = \frac{r}{\mu} \frac{\partial p}{\partial z} \quad (17)$$

We assume that the viscous forces along the axial direction are dominant such that the blood is considered as non Newtonian fluid. Then we solve for velocity  $v_r$  and  $v_z$  with (transmural pressures  $\frac{\partial p}{\partial z} = 0$  and  $\frac{\partial p}{\partial r} = 0$ ) by neglecting inertia forces. The disturbance in the divergent region of the stenosis is caused by a vortex circulation which starts near the wall after the systolic peak when the blood elements begin to decelerate.

For radial direction,

$$v_r^* = \left\{ c_1 b_0 \left[ \frac{Ar}{2} + \frac{A^2 r^3}{16} + \dots \right] + c_2 b_0 \left\{ \left[ \frac{1}{r} - \frac{Ar}{4} - \frac{5}{64} A^2 r^3 + \dots \right] + \left[ \frac{Ar}{2} + \frac{A^2 r^3}{16} + \dots \right] \log r \right\} \times (c_3 \cos Tz + c_4 \sin Tz) \right\} \quad (18)$$

For axial direction,

$$v_z^* = \frac{r^2}{4\mu^*} \frac{\partial p^*}{\partial z} + k_1 \log r + k_2 \quad (19)$$

As the flow of blood is in axial direction, solving for the velocity

$$v_r = u_0 \left\{ c_1 b_0 \left[ \frac{Ar}{2} + \frac{A^2 r^3}{16} + \dots \right] + c_2 b_0 \left\{ \left[ \frac{1}{r} - \frac{Ar}{4} - \frac{5}{64} A^2 r^3 + \dots \right] + \left[ \frac{Ar}{2} + \frac{A^2 r^3}{16} + \dots \right] \log r \right\} \times (c_3 \cos Tz + c_4 \sin Tz) \right\} \quad (20)$$

$$v_z = u_0 \left[ \frac{r^2}{4\mu} \frac{\partial p}{\partial z} + k_1 \log r + k_2 \right] \quad (21)$$

The flux across the stenosed area is computed using the equation [ ] for the rupture case when transmural pressures are appeared along the length of the stenosis in the axisymmetric region. At the prestenotic region the wall shear stress is 20% higher than the one in the unstenotic part. At the downstream, the peak of the wall shear stress appears. Due to the increase in the diastolic phase ( $> 20\%$  as compared at prestenotic region), the inner surface of the wall of the artery undergoes to a very high shear stress (approximately 2.7 times the stress causing a high wall shear stress about 65 dynes/cm<sup>2</sup>). The flux across the stenosed area is computed as

$$Q = 2\pi u_0 \left[ c_1 b_0 \left[ \frac{Ar^3}{6} + \frac{A^2 r^5}{80} + \dots \right] + c_2 b_0 \left\{ \left[ r - \frac{Ar^3}{12} + \dots \right] + \frac{A}{2} \left[ \frac{r^3 \log r}{3} - \frac{r^3}{9} \right] + \dots \right\} \times (c_3 \cos Tz + c_4 \sin Tz) \right] \quad (22)$$

In order to simulate the early phase of the atherogenic process, the analysis on attention has been focused on a slight thickening of the artery intimal layer. The intimal alteration is restricted to a short region of an arterial segment and induces a very mild stenosis with 2% area reduction only. Shear stress evolution in stenosis vessel correlated with the complex rheology of the blood explains the decrease of the vessel circular area in time, wall shear stress

play an important role in remodeling the arterial wall and can lead to arterial thickening, the shear stress at the wall is computed as

$$\tau = \frac{4\mu}{\pi R^4(Z)} 2\pi u_0 \left[ c_1 b_0 \left[ \frac{Ar^3}{6} + \frac{A^2 r^5}{80} + \dots \right] + c_2 b_0 \left\{ \left[ r - \frac{Ar^3}{12} + \dots \right] + \frac{A}{2} \left[ \frac{r^3 \log r}{3} - \frac{r^3}{9} \right] + \dots \right\} \right] \times (c_3 \cos Tz + c_4 \sin Tz)$$

### Results and Discussion

The study of mild stenosis with a reference to rupture case has been analysed. Mathematical model to quantify the hemodynamical effects is studied to explain the various effects of velocity, flux, wall shear stress, the transmural pressures at the proximal wall. The case of rupture of the stenosed region is evident at  $\delta = 0.55$  to  $\delta = 0.853$  mm (71% to 93.14%). It can be noticed from the theoretical analysis that the velocity increases as the stenosis size increases due to the arterial thickening and the flux also increases on the growth of stenosis as irregular form. Computations for velocity, flux and wall shear stress for the case of rupture of mild stenosis indicate that there exists a slight thickening of the intimal layer. For the mathematical investigation the intima layer compliance is restricted to justify the arterial segment induces the mild stenosis by 2% - 5% ( $\delta \ll 1.3$ ). Figures (1), (4) indicate the non linear visco-elastic wall motion which is due to the wall thickness and elasticity varying on transmural pressures. The flux (Fig 8) shows the flow separation close to the wall due to the increase in the wall shear stress at inner surface of the arterial wall. Also the velocity curve (Fig 7) shows the intimal thickening cover the region approximately 1.00 cm long (along the stenosis) and induces 2% of the area reduction. This clearly signifies the occurrence of mild stenosis. The shear stress on the inner surface of the arterial wall (Fig 9) indicates the circulatory system of blood in the stenosed region downstream and upstream, as a result the disturbed effects due to the rupture at the stenosed region describe the saddle shape surface at the systolic phase while in the diastolic phase a very high stress peak occurs and wall shear stress increases at the stenosed region upstream the section. At the upstream (<20% at the prestenotic region) location the flow is observed as laminar and exhibit well-formed parabolic profile. Further near the neck of the stenosis the acceleration of the flow leads to a relatively flat profile and causes high velocity and starts forming separation zone. Therefore due to the rupture at the stenosed region the shear rate of the stenosis causes a great shearing action on the inner surface at the wall. The conclusive evidence such as a vortex circulation occur due to the rupture of the mild stenosis, the recirculation flow can induce on the wall on high shear stress and decreases at the rupture stage and the end stenotic region (in the axial direction), it can be subjected to very different shearing action.



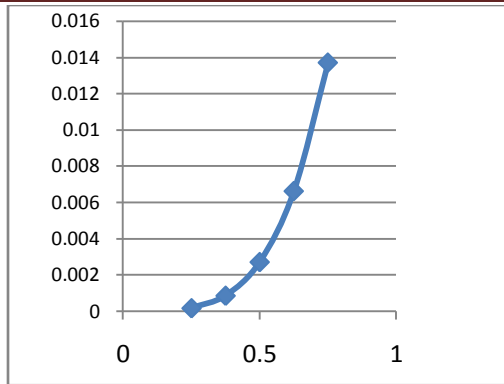


**Fig (1) Radius v/s Rupture coefficient  
 0.00016953**

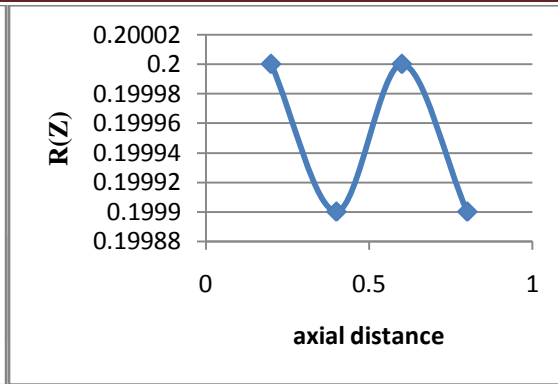
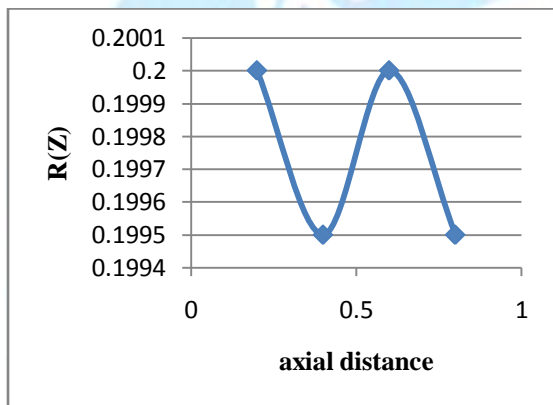


**Fig (2) axial distance v/s R(z) for m =**



**Fig(3) axial distance v/s R(Z) for m = 0.00085825**

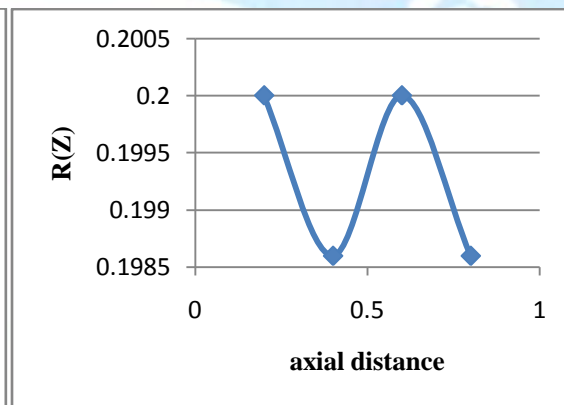


**Fig (4) R(Z) for m =0.0027125**

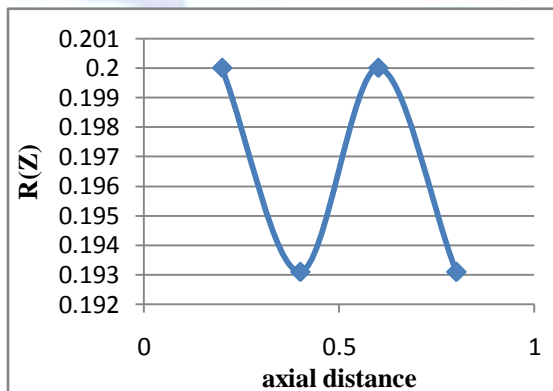


**Fig (5) axial distance v/s R(Z) for m =0.0066223  
 =0.0137**

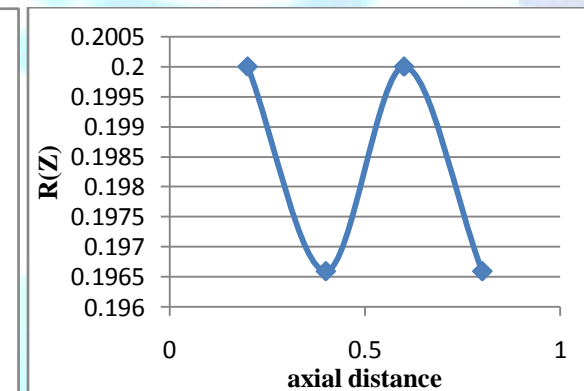


**Fig (6) axial distance v/s R(Z) for m**

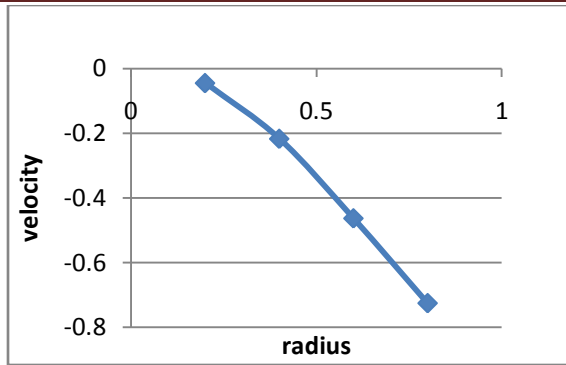


Fig (7) radius v/s velocity

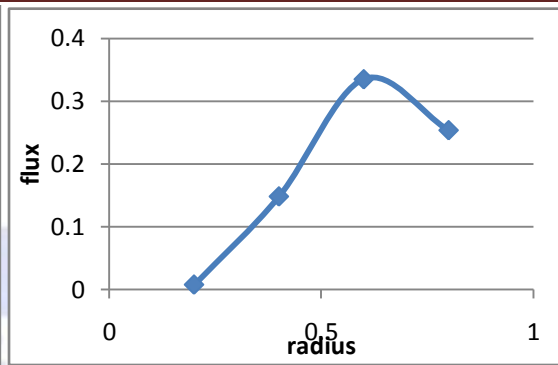


Fig (8) radius v/s Flux

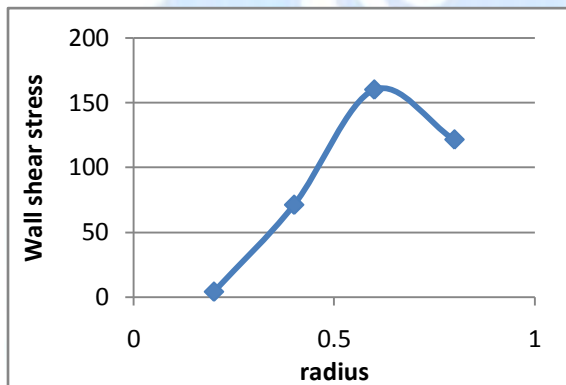


Fig (9) radius v/s Wall Shear Stress

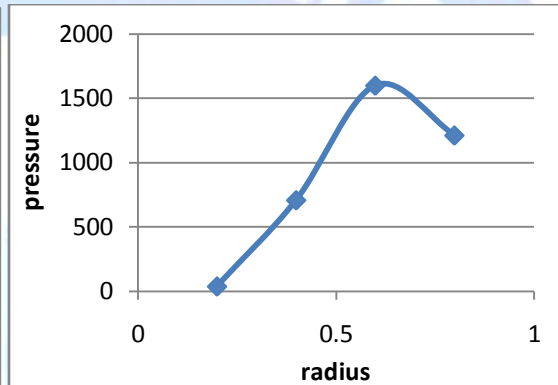


Fig (10) radius v/s Pressure



**NOMENCLATURE**

- R(z) – surface distance of stenosis from the axis of the artery
- R<sub>0</sub> – initial radius of the stenosed area
- δ<sub>v</sub> - thickness of stenosis
- z- axial distance
- z<sub>i</sub> – axial distance at i = 0.2,0.4,0.6,0.8
- Z<sub>0</sub> – initial axial distance
- ρ - density
- v – velocity
- p(z) pressure
- μ - coefficient of viscosity
- t – time
- τ- shear stress
- τ<sub>wss</sub> - wall shear stress.
- v<sub>r</sub> – radial velocity
- v<sub>z</sub> – axial velocity
- Q- flux
- m<sub>i</sub> – rupture coefficient
- G<sub>0</sub> – pressure due to heat that remains to drive the pipe flow
- ϑ - kinematic viscosity
- D – diameter
- r – radius
- θ - amplitude
- c<sub>1</sub>,c<sub>2</sub>, c<sub>3</sub> ,c<sub>4</sub>, b<sub>0</sub>, A,u<sub>0</sub>, k<sub>1</sub>, k<sub>2</sub> - constants

$$Q = \int_0^R 2\pi r v_r dr$$

$$\tau = \frac{4\mu Q}{\pi R^4(Z)}$$

## REFERENCES

1. Back.L, Cho.Y, Crawford D and Cuffel R [1984], 'Effect of mild atherosclerosis on flow resistance in a coronary artery casting of man', J. Biomech. Engng 106, 48-53.
2. Liepsch D [1998], 'Flow visualization and 1 and 3-D Laser Doppler anemometer measurements in models of human carotid arteries', Clinical Hemorheology and Microcirculation, Vol. 18, 1-30.
3. Baaijens J P W, Van Steenhoven A A and Janssen J D [1993], 'Numerical analysis of a steady generalized Newtonian blood flow in a 2-D model of the carotid artery bifurcation', Biorheology, Vol. 13, 63-74.
4. Liepsch D and Zimmr R [1995], 'The dynamics of pulsatile flow in distensible model arteries', Technology and Health care, Vol. 3, 185-199.
5. Kaluzynski K and Liepsch D [1995], 'The effect of wall roughness on velocity distribution in a model of the carotid sinus bifurcation- analysis of laser and ultrasound Doppler velocity data', Technology and health care, Vol. 3, 153-159.
6. Katiyar [2000], 'The pulsatile flow of blood in an elastic tube with wall deformation', J. Applied Sciences and Computations.
7. David A Steinman, Tamie Poepping , Muro Tambasco, Richard N Rankin and David W Holdsworth [2000], ' Flow patterns at the Stenosed cartotid bifurcations: effect of concentric versus Eccentric stenosis', J. Analysis of Biomedical Engineering, Vol.28, 415-423.
8. Basavarajappa [2002], 'The experimental and numerical analysis of pulsatile flow in carotid artery bifurcations'.
9. J.C Mishra, S. Maiti, "Peristaltic pumping of blood through small vessels of varying cross section".